Received: 6 September 2021 | Revised: 12 November 2021 | Accepted: 14 December 2021

DOI: 10.1111/jam.15416

Journal of Applied Microbiology sfam

ORIGINAL ARTICLE

Comparative survival of environmental and clinical *Mycobacterium abscessus* isolates in a variety of diverse host cells

Charmie K. Vang[1] | **Stephanie N. Dawrs**[1] | **Nicole M. Oberlag**[2] | **Anah E. Gilmore**[3] | **Nabeeh A. Hasan**[1] | **Jennifer R. Honda**[1]

[1]Center for Genes, Environment and Health, National Jewish Health, Denver, Colorado, USA

[2]Department of Biology, Harvey Mudd College, Claremont, California, USA

[3]Professional Biomedical Science Program, University of Denver, Denver, Colorado, USA

Correspondence
Jennifer R. Honda, Center for Genes, Environment and Health, National Jewish Health, Denver, CO, USA.
Email: HondaJ@njhealth.org

Funding information
Padosi Foundation

Abstract

Aims: *Mycobacterium abscessus* subsp. *abscessus* (MABS) is an emerging, opportunistic pathogen found globally in freshwater biofilms and soil. Typically, isolates are treated as a uniform group of organisms and very little is known about their comparative survival in healthy host cells. We posit that environmentally- and clinically derived isolates, show differential infectivity in immune cells and resistance to innate defenses.

Methods and Results: Six MABS isolates were tested including three water biofilm/soil and three sputum-derived isolates. A clinical MABS type strain and an environmental isolate of *Arthrobacter* were also included. MABS counts were significantly higher compared to *Arthrobacter* after co-culture with *Acanthamoeba lenticulata*, BEAS-2B epithelial cells, alveolar macrophages and the THP-1 macrophage cell line. A rough sputum-derived MABS isolate emerged as an isolate with higher virulence compared to others tested, as both a pellicle and cord former, survivor in the human cell models tested, inducer of high and prolonged production of pro-inflammatory cytokines, and the capacity to evade LL-37.

Conclusions: Findings support intraspecies variation between MABS isolates.

Significance and Impact of the Study: These data indicate subversion of host immune defenses by environmental and clinical MABS isolates is nuanced and maybe isolate dependent, providing new information regarding the pathogenesis of NTM infections.

KEYWORDS

environmental, immunology, microbial-cell interaction, nontuberculous mycobacteria, virulence

Charmie K. Vang and Stephanie N. Dawrs contributed equally to this work and share first authorship. First author order was determined by a best out of three coin toss.

INTRODUCTION

Mycobacterium abscessus subsp. *abscessus* (MABS), reclassified in 2018 as *Mycobacteroides abscessus* subsp. *abscessus* (Gupta et al., 2018), is widely recognized to cause opportunistic pulmonary infections in predisposed hosts (Cook, 2010). Infections can also arise at surgical sites, cause cellulitis of the breast, foot infections, peritonitis related to peritoneal dialysis catheters, parotitis and eye infections (Ciampa & Wong, 2021; Imam et al., 2021; Kim et al., 2020; Patel et al., 2021; Wojcik et al., 2021; Yonekawa et al., 2020). Recent studies suggest promising roles for bacteriophages and inhaled nitric oxide in the fight against stubborn MABS infections (Bogdanovski et al., 2020; Dedrick et al., 2019; Lobocka et al., 2021).

Environmentally adaptable and consistently in our surroundings (Falkinham, 2009), MABS is regarded as an emerging and worrisome global pathogen of nightmare proportions (Lopeman et al., 2019; Nessar et al., 2012). This scenario is especially true for people with cystic fibrosis (pwCF) (Degiacomi et al., 2019; Martiniano et al., 2019). As cases continue to rise, it's paramount to understand MABS biology by elucidating their capacity to interact with healthy host cells.

By the current paradigm, pulmonary MABS infections are associated with environmental exposures, but reports suggest the potential for person-to-person transmission of MABS in pwCF, fostering renewed interest in the prevalence of environmental MABS in healthcare systems (Bryant et al., 2013). However, isolation and identification of MABS from the environment remains challenging and environmental MABS isolate collections are uncommon and sought-after. This scarcity reduces our ability to compare virulence between water biofilm and soil MABS isolates to clinical MABS isolates, leaving a severe and consequential gap in the current knowledge of MABS pathogenesis.

Within our studies of nontuberculous mycobacteria (NTM) in the US geographic hot spot of Hawai'i, we have demonstrated recovery of viable MABS from a variety of built and natural environments (Honda et al., 2016; Virdi et al., 2021). From this collection, a panel of environmental and clinical MABS was studied to fill in the current knowledge gaps of understudied environmental MABS isolates. Specifically, we investigate the consequence of MABS infection using a variety of microbiological criteria and assess survival in an assortment of innate immune cells including amoebae, human airway epithelial cells, and macrophages and interrogate the panel's resistance to a host-protective antimicrobial peptide (AMP). As an added comparison, the MABS type strain ATCC 19977 and a common soil commensal, *Arthrobacter sp*., also isolated from the Hawai'i environment, were included. These studies shed new light on the interactions between environmental and clinical MABS isolates and the host innate immune defenses involved in the pathogenesis of MABS infections.

MATERIALS AND METHODS

Bacteria

Eight bacterial isolates derived from environmental or clinical samples were tested (Table 1). Isolates 1–3 and 5–8 were identified as MABS and Isolate 4 was identified as *Arthrobacter sp*. as determined by Sanger sequencing of a partial region in the *rpoB* gene as we have published (Honda et al., 2016; Virdi et al., 2021). The MABS type strain ATCC 19977 was included as a positive control (Isolate 7). Isolates were cultured in Middlebrook 7H9

TABLE 1 Bacterial isolates

Isolate no.	Isolate ID	Source	Sample origin	Location	Species	Smooth or rough
Isolate 1	19-KPH-39	Clinical	Sputum	Oahu, Hawai'i	MABS	Smooth
Isolate 2	19-KPH-67	Clinical	Sputum	Oahu, Hawai'i	MABS	Rough
Isolate 3	18-M-SD-2-A2-1-37	Environmental	Residential showerhead biofilm	Hawai'i Island, Hawai'i	MABS	Smooth
Isolate 4	18-KAR-4-1-22	Environmental	Fresh stream water filter	Oahu, Hawai'i	*Arthrobacter sp.*	N/A
Isolate 5	241-1-MG30	Environmental	Soil	Hawai'i Island, Hawai'i	MABS	Smooth
Isolate 6	234-2MG30	Environmental	Soil	Hawai'i Island, Hawai'i	MABS	Smooth
Isolate 7	ATCC 19977	Clinical	Type strain; human knee	St. Louis, Missouri	MABS	Smooth
Isolate 8	205	Clinical	Sputum	Oahu, Hawai'i	MABS	Mixed

N/A, not applicable.

broth supplemented with 10% albumin dextrose catalase (ADC) enrichment, 0.2% glycerol, and 0.05% Tween 80 referred herein as "7H9 broth." Growth of MABS isolates and *Arthrobacter* were indistinguishable on Middlebrook 7H10 agar plates.

DNA isolation, PCR and sequencing

Intact genomic DNA was extracted according to Epperson and Strong (2020) including the optional bead-beating step. The PCR amplification and sequencing targeted an approximately 700 bp segment of the RNA polymerase Region Five beta subunit *rpoB* gene (Adekambi et al., 2003; Telenti et al., 1993). PCR reactions with 1–10 ng of template DNA, 2 μl each of 5 μM forward and reverse *rpoB* primers and nuclease free water were combined in 96-well plates and submitted for Sanger sequencing (Quintara Biosciences, San Francisco, CA).

rpoB sequence analyses and phylogeny

Taxonomic identification of isolates was conducted through *rpo*B sequence analysis (Adekambi et al., 2003; Telenti et al., 1993). Sequences were trimmed for quality by removing low-quality base calls at the beginning and end of each sequence and then comparing the sequences against *rpoB* type strain sequences using the BLAST algorithm. Quality trimmed *rpo*B sequences from all isolates were aligned and compared using MEGA (Stecher et al., 2020). A phylogenetic tree based on *rpo*B sequence variation was constructed by the neighbour-joining method. The phylogeny was evaluated by a bootstrap analysis based on 1000 replicates of the observed single-nucleotide polymorphisms (SNPs).

Data availability statement

*rpo*B sequences were deposited in the National Center for Biotechnology Information (NCBI) in GenBank under accession numbers MZ401476–MZ401483.

Colony morphology assessments

Isolates were streaked for isolation onto Middlebrook 7H10 plates and incubated for 3–5 days at 37°C. We discovered that *Arthrobacter sp*. did not grow at 37°C; therefore, it was primarily cultured at 22°C (as explained in Results). Individual colony morphology was visualized and documented under a dissecting microscope at a total magnification of 40× (Ken-A-Vision). MABS isolates with uniform smooth, round morphologies were classified as "smooth." Isolates with uniform wrinkled or textured edges were classified as "rough" as assessed by three independent technicians.

Pellicle formation assay

Isolates were streaked onto 7H10 plates and incubated for 3–5 days at 37 or 22°C for *Arthrobacter sp*. A single colony of each isolate was picked and inoculated into 5 ml of 7H9 broth and stagnantly incubated at 37°C (or 22°C for *Arthrobacter sp*.) for 23 days. Pellicle formation was determined by visibly notable bacterial aggregation at the air-liquid interface of the culture tube.

Total lipid extraction and thin-layer chromatography

Methods for total lipid extraction and thin-layer chromatography (TLC) are published (Honda et al., 2019). In brief, isolates were cultured in Proskauer–Beck (PB) media and total lipids were extracted from bacterial pellets using 1:1 $CHCl_3$:MeOH (chloroform:methanol). Lipid extraction was repeated three times, each time pooling the supernatants to collect the soluble lipid fractions, and evaporated using N_2. For TLC, lipid fractions were resuspended in 2:1 $CHCl_3$:MeOH and vortexed. 25 μl of each lipid fraction was spotted onto silica plates (HPTLC Silica gel 60 F_{254}; Merck KGaA) and 65:24:4 $HCCl_3$:MeOH:H_2O (v/v/v) was used to separate the lipid species. Total lipids were visualized with $CuSO_4$ charring spray under heat.

7H9 broth growth assay

MABS (1×10^6) or *Arthrobacter* were inoculated in 1 ml 7H9 broth in low-bind tubes and incubated on a rotary shaker at 37°C. CFU were quantified at 1, 24, 48 and 96 h post inoculation by plating serial dilutions on duplicate onto 7H10 plates with incubation at 37°C until visible growth was observed. *Arthrobacter* showed no growth at 37°C; thus, identical experiments were performed but with culture incubation on a rotary shaker at 22°C and 7H10 plate incubation at 22°C.

Acanthamoeba lenticulata co-culture

Maintenance: *Acanthamoeba lenticulata* ATCC 30841 trophozoites were cultured in sterile peptone-yeast-glucose

(PYG) broth (no antibiotics/antimycotics) at 22°C for maintenance cultures. To prevent amoebae overgrowth and encystment, maintenance cultures were centrifuged, spent medium was removed and fresh PYG was added every fourth passage day (Hasan et al., 2021).

Culture media growth assay: 1×10^5 MABS or *Arthrobacter sp*. were inoculated in 1 ml PYG media in 6-well tissue culture plates and incubated at 22°C. CFU was manually quantified at 1, 24, 48 and 96 h post PYG inoculation (in the absence of amoebae) in duplicate by plating serial dilutions of the cultures onto 7H10 plates. Plates were incubated at 22°C for 3–5 days.

Acanthamoeba lenticulata co-culture: All amoebae co-culture experiments were performed at 22°C. *A. lenticulata* was co-cultured with the isolate panel using a MOI of 1:1 in 6-well tissue culture plates. After one hour of co-culture, unphagocytosed bacteria were removed by aspiration and washed with 1× PBS. Amoebae in the 1 h wells were lysed using 0.025% SDS and 7H9 plating solution (2.35 gl^{-1} Middlebrook 7H9 base, 0.1% Tween 80, 10% OADC supplement). Lysates were serially diluted and plated in duplicate on 7H10 plates. Fresh PYG media was added to the remaining wells for continued incubation at 22°C until 24, 48 and 96 h of co-culture which were processed as described for the 1-h timepoints.

BEAS-2B airway epithelial cell co-culture

BEAS-2B cells were seeded at 2×10^5 in fibronectin-collagen coated T-75 flasks and maintained in BronchiaLife cell culture media (Lifeline Cell Technologies) supplemented with gentamycin (Lifeline Cell Technologies). Cells were incubated at 37°C, 5% CO_2 with humidity with media changes occurring every 2–3 days and passaging every 5–7 days once cells reached ~80% confluency. Cells were seeded at 1×10^5 cell per well in fibronectin-collagen coated 12-well cell culture plates and expanded for 3 days to reach approximately 5×10^5 per well. Cells were co-incubated with the isolate panel at a MOI of 1:1 and similarly processed to other cells referenced above. Culture supernatants were filtered and saved for downstream cytokine analyses.

Primary human alveolar macrophage co-culture

Primary human alveolar macrophages (AM) were obtained from fresh bronchial lavage fluid collected from recently deceased human donor lungs. Methods used for AM and isolate co-culture are published (Honda et al., 2019). Similar to BEAS-2B cells, culture supernatants were filtered and saved for downstream analyses.

Ethics statement: AM were procured from the National Jewish Health (NJH) Human Lung Tissue Consortium that regularly obtains donors lungs from non-smokers through the International Institute for the Advancement of Medicine and the National Disease Research Interchange and Donor Alliance. Samples are not suitable for transplantation and donated for medical research. This consortium has IRB exemption to allocate de-identified AM to NJH investigators.

THP-1 macrophage co-culture and acid fast staining staining

THP-1 media growth assay: The growth media used for THP-1 cells is comprised of RPMI 1640 (Fisher), supplemented with 10% FBS and 1% antibiotic/antimycotic (Gibco). This antibiotic/antimycotic is comprised of 10,000 units/ml of penicillin, 10,000 μg/ml of streptomycin and 25 μg/ml of Fungizone. As with 7H9 broth and PYG culture media, the isolate panel was cultured in THP-1 culture media (in the absence of host cells) using the same parameters discussed above.

THP-1 co-culture and acid fast staining staining: THP-1 macrophages were co-cultured with individual isolates from the panel as published (Honda et al., 2019) and culture supernatants were filtered and saved for downstream analyses. In parallel, THP-1 macrophages were seeded at a density of 1×10^5 cells in 4-well chamber slides (Nunc, Lab-Tek II chamber slides) to perform acid fast staining (AFB). Cells were fixed in ice-cold methanol and placed into a −20°C freezer for 8 min (Hobro & Smith, 2017). After 8 min, methanol was removed, cells were washed in 1X PBS, and air-dried. Once dry, cells were stained for AFB using the Kinyoun cold method (Hardy Diagnostics) and visualized by light microscopy at a total magnification of 1000X (SeBa, Laxco).

Quantification of immune mediators from BEAS-2B, AM and THP-1 culture supernatants

ELISA and Multiplex: BEAS-2B and AM cell culture supernatants were filtered through a 0.2 μm filter and assayed for TNFα by ELISA following the manufacturer's instructions (R&D Systems). THP-1 cell culture supernatants were filtered through a 0.2 μm filter for cytokine/chemokine analyses on the Quanterix Simoa Multiplex platform for TNFα, IL-6, IL-8, IL-10 and IL-1β (Children's Hospital, Colorado).

LL-37 kill assay

MABS LL-37 kill assay was performed as published to test the resistance of the isolate panel to 0, 25, or 150 μg/ml of synthetic LL-37 peptide (Honda et al., 2015, 2019). Briefly, MABS isolates were incubated on a rotary shaker at 37°C. *Arthrobacter* LL-37 assays were performed at both 37 and 22°C. Changes in CFU were monitored 1, 24, 48 and 96 h post inoculation. To assess whether exposure to NTM neutralized the antimicrobial activity of LL-37, 96-h cultures were pelleted at 6000 *g* and the supernatants were transferred to new sterile low-bind tubes. 2×10^5 *Escherichia coli* were inoculated into the supernatants and incubated at 37°C on a rotary shaker (Honda et al., 2015, 2019). After 4 h, *E. coli* was streaked onto Luria Britani agar plates, incubated at 37°C overnight, and inspected for *E. coli* viability in a LL-37 bioassay.

Statistics

Data were analysed with GraphPad 9 using paired *t*-tests or two-way analysis of variance (ANOVA) to determine statistical significance for CFU assays. Data are expressed as means ± SEM for three or more independent determinations for each experimental point. For some statistical considerations, environmental MABS isolates (i.e. Isolates 3, 5, 6) were grouped and clinical isolates (i.e. Isolates 1, 2, 7, 8) were grouped and the *Arthrobacter* data were analysed separately. Two-way ANOVA with Dunnett's or Tukey's multiple comparisons test was used for TNFα ELISA. Values with $p < 0.05$ were considered statistically significant.

RESULTS

Genetic analysis and microbiology of the isolate panel

To measure the genetic similarity among the isolate panel, *rpoB* gene sequence variation was analyzed. Phylogenetic analyses identified the taxonomy of all isolates as MABS, which were genetically similar to each other and to the MABS ATCC 19977 type strain, with the exception of Isolate 4. Isolate 4 was identified as *Arthrobacter sp*. (Figure 1a).

MABS demonstrates "smooth" or "rough" colony morphologies that are related to virulence (Byrd & Lyons, 1999). To establish differences in colony morphology, MABS isolates were streaked for isolation onto 7H10 agar. MABS with "smooth" morphology were Isolates 1, 3, 5, 6 and 7. Isolate 2 was classified

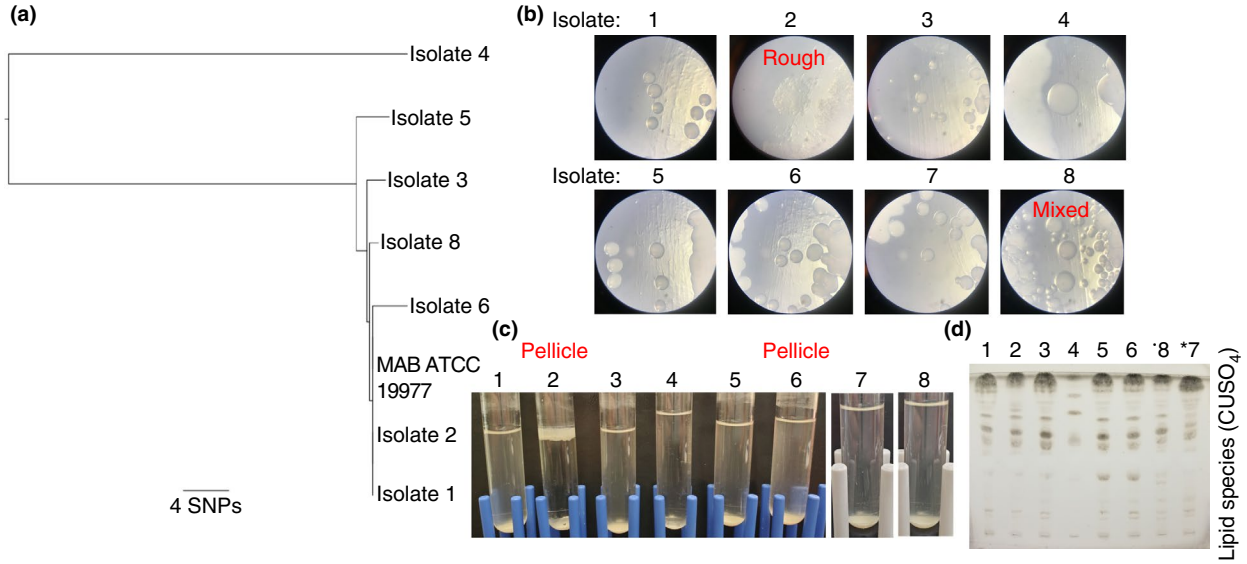

FIGURE 1 Isolate panel characteristics. (a) Phylogenetic analyses of isolates used in this study. A phylogeny based on the multiple sequence alignment of partial *rpoB* sequences inferred between isolate relationships was obtained using the neighbor-joining method and observed SNPs. The scale bar represents a 4 SNP difference in nucleotide sequences. (b) Colony morphology of the isolate panel after streaking for isolation on Middlebrook 7H10 agar plates and viewed under a dissecting scope. Total magnification = 40X. (c) Pellicle formation was assessed after incubation for 23 days in Middlebrook 7H9 broth culture. Isolates that produced observable bacterial aggregation at the air-liquid interface of the culture were determined to have formed a pellicle. (d) TLC of total lipid extracts from the isolate panel. 25 μl of each sample were spotted onto 13 × 10 cm analytical TLC plates and eluted in 65:25:4 $HCCl_3$:MeOH:H_2O. Total lipids were visualized with CuSO4. Isolate 4 = *Arthrobacter sp*

as a "rough" MABS isolate and Isolate 8 was determined to be of mixed morphology (Figure 1b, Table 1). *Arthrobacter* (Isolate 4) demonstrated smooth colonies on 7H10 agar. The ability to grow at the air–liquid interface in 7H9 broth was used as a read-out for pellicle formation. Of the eight isolates, pellicles were observed for Isolates 2 and 6 (Figure 1c). The pellicle of Isolate 2 was thick and buff-white and was firmly adherent to the tube's inner surface. Conversely, the pellicle of Isolate 6, while visible to the naked eye, was fragile because it floated on the liquid surface and was easily dislodged upon movement of the tube. Next, total lipids were extracted from the isolate panel and compared using TLC. The lipid diversity of *Arthrobacter* was notably different than the lipid profiles of the MABS isolates (Figure 1d).

Growth of the isolate panel in culture media, no host cells

Isolates were inoculated into 7H9 broth, incubated at 37°C and changes in CFU monitored 1, 24, 48 and 96 h after inoculation to monitor differences, if any, in the growth of the isolates in standard mycobacterial culture media in the absence of host cells. All MABS isolates showed comparable growth in culture over time, but with some timepoint differences. The growth of both environmental soil Isolates 5 and 6 were significantly higher compared to clinical Isolate 8 at 24 h. By the 48- and 96-h timepoints, clinical Isolate 2 demonstrated significantly lower CFU counts in 7H9 broth compared to soil Isolate 5. *Arthrobacter* did not grow at any of the timepoints tested (Figure 2a). To determine whether this was due to the

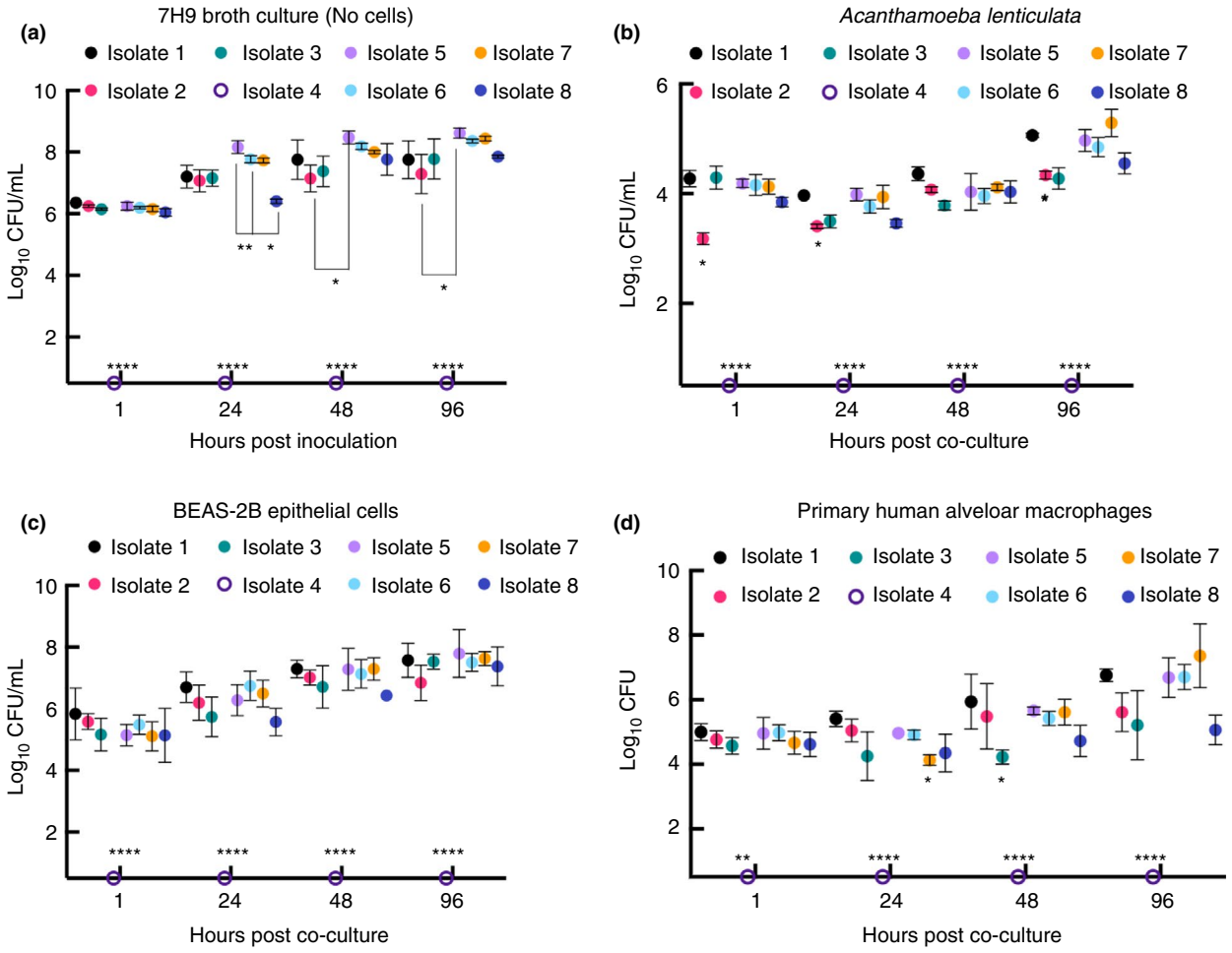

FIGURE 2 Growth of the isolate panel in culture media and a variety of host cells. (a) Growth curve of the isolate panel in Middlebrook 7H9 broth incubated at 37°C. CFU were quantified at 1, 24, 48 and 96 h post inoculation. $n = 3$ independent experiments. *$p < 0.05$; **$p < 0.005$; ****$p < 1 \times 10^{-16}$. (b) Co-culture of the isolate panel with *Acanthamoeba lenticulata*. 1×10^5 *A. lenticulata* and a MOI 1:1 were used. CFU were quantified at 1, 24, 48 and 96 h post infection. Amoebae co-culture was performed at 22°C. At least 3 independent experiments were performed for all isolates. *$p < 0.05$ (comparing Isolate 1 vs 2); ****$p < 1 \times 10^{-16}$. (c) The isolate panel was co-cultured with 2×10^5 BEAS-2B airway epithelial cells using a MOI 1:1. CFU were quantified at 1, 24, 48 and 96 h post inoculation. **$p < 0.005$, ****$p < 1 \times 10^{-16}$. (d) 1×10^6 primary human alveolar macrophages were co-cultured *ex vivo* with the isolate panel using a MOI 1:1. CFU were quantified at 1, 24, 48 and 96 h post inoculation. *$p < 0.05$; **$p < 0.005$; ****$p < 1 \times 10^{-16}$. Isolate 4 = *Arthrobacter sp.*

viability of *Arthrobacter*, two 7H9 *Arthrobacter* cultures were incubated at either 37 or 22°C. *Arthrobacter* demonstrated robust growth only when cultured and plated at 22°C (Figure S1a).

Co-culture of isolates with *Acanthamoeba lenticulata*

The relationship between NTM and environmental amoebae has been reported, but is not widely studied for MABS (Adékambi et al., 2006; Thomas & McDonnell, 2007). When inoculated in amoebae PYG culture media in the absence of amoebae, the majority of the MABS isolates showed sustained viability across all the timepoints tested. However, significantly less CFU was recovered for Isolate 8 compared to Isolate 1 at 24 h and Isolates 6 and 7 at 96 h post inoculation. In this culture media, *Arthrobacter* grew significantly better than all MABS isolates (Figure S1b).

To assess the capacity of environmental and clinical MABS to survive in amoebae, cultures of *A. lenticulata* were co-cultured with MABS or *Arthrobacter* at 22°C to avoid amoebae encystment. Changes in CFU were monitored at 1, 24, 48 and 96 h post co-culture. The majority of the MABS isolates demonstrated sustained survival in the presence of *A. lenticulata* with the exception of Isolate 2. Significantly less numbers of Isolate 2 were recovered from *A. lenticulata*. Overall, *A. lenticulata* controlled *Arthrobacter* replication at each timepoint tested (Figure 2b).

Co-culture of isolates with human lung epithelial cells and macrophages

In BEAS-2B epithelial cells, all seven MABS isolates demonstrated equivalent and sustained growth overtime that was significantly higher compared to *Arthrobacter* at each timepoint tested (Figure 2c) and no significant differences in CFU were observed when the isolates were grouped and analysed based on their stratification as environmental ($n = 3$) or clinical ($n = 4$) MABS isolates (Figure S2a).

To study the consequence of MABS infection in human macrophages, primary human AMs were co-cultured with the isolate panel *ex vivo*. Similar to BEAS-2B cells, equivalent and sustained growth was observed among all seven MABS isolates that was significantly higher than the *Arthrobacter* isolate (Figure 2d). However, the MABS ATCC 19977 type strain (Isolate 7) showed significantly less CFU 24 h after co-culture with AM compared to clinical MABS Isolate 1 and environmental soil Isolates 5 and 6. By 48 h, significantly less CFU were recovered from AM infected with Isolate 3 recovered from a water biofilm swab compared to soil-derived MABS Isolates 5 and 6. Yet, no differences in CFU were observed when the MABS isolates were categorized as clinical or environmental at any of the timepoints tested (Figure S2b).

To assess the survival of the isolate panel in a different macrophage model, the human monocytic cell line THP-1 was differentiated into macrophages using PMA. No differences in CFU were observed when the MABS isolates were categorized as clinical or environmentally derived (Figure S2c), but MABS survival in THP-1 cells were significantly higher than *Arthrobacter* (Figure 3a). Acid-fast bacilli (AFB) staining show red-stained carbofuschin positive MABS in the context of THP-1 cells identified by methylene blue-stained nuclei (Figure 3b). Not surprising, AFB positive bacilli were absent from THP-1 cells infected with *Arthrobacter*, a Gram-positive bacterium. Light microscopy studies revealed Isolate 2 as a cord former (Figure 3c) and is consistent with Isolate 2 as a pellicle former (Figure 1c). In comparison, cording was not observed for any of the other isolates including *Arthrobacter* or the MABS representative, Isolate 5 (Figure 3c).

Data shown in Figure S1a suggest *Arthrobacter* is sensitive to 37°C temperatures compared to ambient temperature (22°C). To investigate whether the reduction in *Arthrobacter* was due to macrophages or incubation temperature, the isolate panel was inoculated into THP-1 culture media alone in the absence of cells at 37°C. *Arthrobacter* was not recovered from any of the timepoints tested (Figure S1c). The number of CFU for MABS Isolates 1, 2, 3 declined with extended culture in THP-1 media by the 48-h timepoint and Isolates 5, 6 and 8 also declined by the 96-h timepoint. Isolate 7 demonstrated sustained growth at all timepoints (Figure S1c). To test whether control of *Arthrobacter* was due to antimycotic and antibiotic in the THP-1 culture media, *Arthrobacter* and the MABS ATCC 19977 type strain Isolate 7 were incubated separately in the presence of THP-1 culture media with and without antibiotics/antimycotics at 22°C. Isolate 7 showed equivalent CFU in either media at 22°C; whereas, viable growth of *Arthrobacter* was only observed in THP-1 media without antibiotics/antimycotics at this temperature (Figure S1d).

Immune responses to clinical or environmental MABS compared to *Arthrobacter*

TNFα release by *Arthrobacter*-infected BEAS-2B cells (Figure 4a) and *Arthrobacter*-infected AM (Figure 4b) 24 h after infection trended higher than TNFα levels recorded for the MABS isolates when grouped. To further understand the host immune response to infection, multiple analyte testing

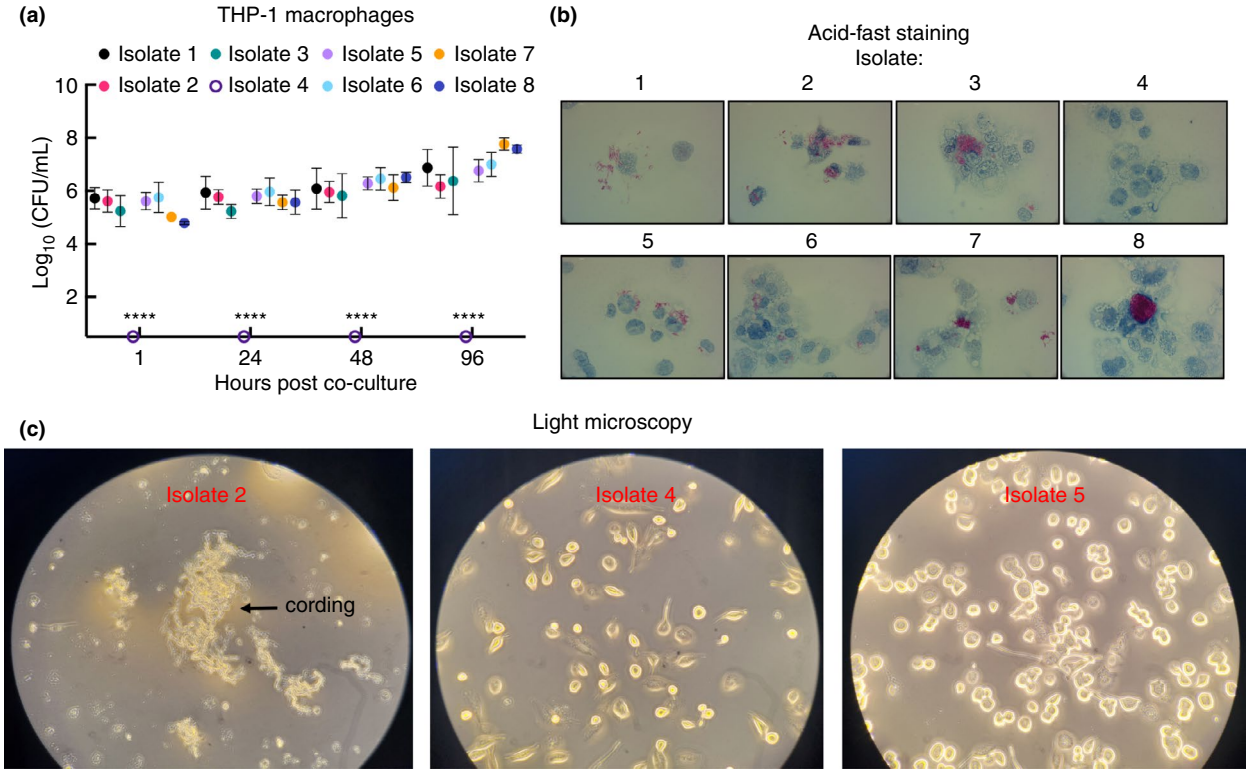

FIGURE 3 Co-culture of the isolate panel with human THP-1 macrophages. (a) 1×10^6 THP-1 were co-cultured with the isolate panel using a MOI 1:1. CFU were quantified at 1, 24, 48 and 96 h post inoculation. ****$p < 1 \times 10^{-16}$. $n = 6$ independent experiments. (b) 1×10^5 THP-1 macrophages were co-cultured with the isolate panel using a MOI 1:1 in 4-well chambers slides. At 48 h post co-culture, cells were fixed, AFB stained, and imaged by light microscopy (total magnification 1000×). (c) Visualization of cultures was performed 96 h post inoculation after washing the cell monolayer with 1× PBS using light microscopy. Representative images of Isolates 2, 4 and 5 are shown (total magnification 200×). Arrow for Isolate 2 indicates examples of MABS cords. These co-culture experiments were performed at 37°C. Isolate 4 = *Arthrobacter sp*

was performed on THP-1 culture supernatants collected at the 24, 48 and 96-h timepoints that included quantification of the chemokine IL-8, anti-inflammatory molecule IL-10, pleotropic molecule, IL-6, and pro-inflammatory mediators IL-1β and TNFα. Overall, IL-8 levels remained low and unchanged at all three timepoints tested for all MABS isolates and *Arthrobacter* (Figure 4c–e). At the isolate level, THP-1 cells produced higher and sustained levels of the pro-inflammatory cytokines IL-6, IL-1β and TNFα in response to MABS Isolate 2 compared to the other isolates tested (Figure 4c–e). When categorized together, analyte production was higher among the clinical MABS isolates compared to the environmental MABS isolates and more comparable to *Arthrobacter* (Figure S3a–c).

Evasion against a host-protective AMP

Cathelicidin, *a.k.a.*, LL-37, is an endogenous AMP produced by a variety of innate immune cells that potently kills bacteria such as *E. coli* (Durr et al., 2006; Honda et al., 2015; Lehrer & Ganz, 2002; Zanetti, 2004). Resistance to and inactivation of LL-37 has been reported as a novel virulence mechanism of NTM (Honda et al., 2015, 2019). To assess resistance to LL-37, the isolate panel was incubated with 0, 25 or 150 μg/ml of LL-37 and changes in CFU monitored at 37°C at 1, 24, 48 and 96 h after incubation as we have published (Honda et al., 2015, 2019). Generally, LL-37 was ineffective at killing any of the MABS isolates (1, 3, 5, 6, 7 and 8) in the presence of 25 or 150 μg/ml of LL-37 at 24 and 48 h (data not shown) or at 96 h post inoculation (Figure 5a,b). Of interest, while CFU counts for Isolate 2 were lower than the other MABS isolates, counts trended higher in the presence of 25 or 150 μg ml^{-1} of LL-37 at 96 h post exposure (Figure 5a,b). As before, *Arthrobacter* did not grow at this incubation temperature. To further investigate the susceptibility of *Arthrobacter* to LL-37, the LL-37 assay was repeated for *Arthrobacter* incubated at 37 or 22°C (Figure S4a,b), confirming growth of the isolate at this temperature and sensitivity to LL-37.

To assess whether NTM inactivates the antimicrobial activity of LL-37, we apply a biological read-out assay. In these assays, surrogate bacteria like *E. coli* are incubated with LL-37 in the presence or absence of NTM isolates.

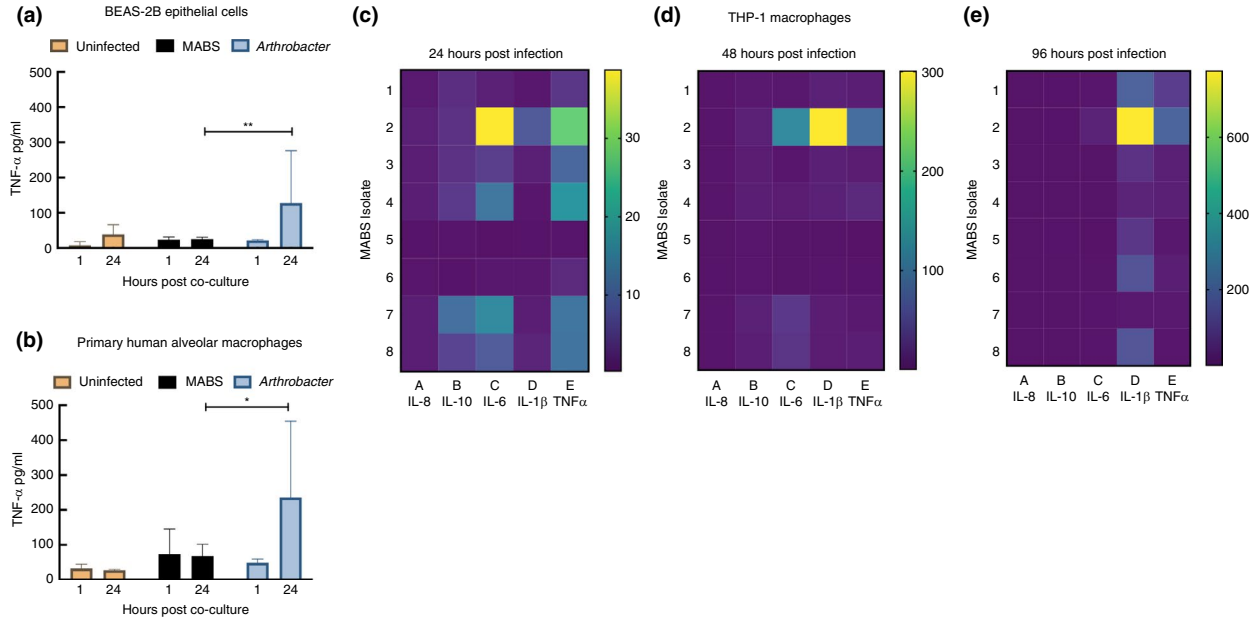

FIGURE 4 Co-culture of the isolate panel with healthy human epithelial cells or macrophages and cytokine/chemokine quantification. (a) TNFα quantification of BEAS-2B culture supernatants 1 or 24 h post culture. $^{**}p = 0.0041$. (b) TNFα quantification of alveolar macrophage culture supernatants 1 and 24 h post culture. $^{*}p = 0.0112$. For CFU, at least 3 or more independent experiments were performed for all isolates and for each cell type. For ELISA, $n = 2$ was performed for each cell type. These co-culture experiments were performed at 37°C. Multiple analyte analyses of THP-1 culture supernatants. Culture supernatants from THP-1 co-culture experiments after 24, 48 and 96 h detailed in this figure were collected and filtered through a 0.2 μm filter. IL-8, IL-10, IL-6, IL-1β and TNFα were quantified on the Quanterix Simoa Technology platform. 24-h results are shown in (c), 48-h results are shown in (d), and 96 h results are shown in (e). $n = 3$ independent experiments per timepoint. Values are represented as the pg/ml cytokine level divided by the THP-1 uninfected cell supernatant pg/ml value at that timepoint. Median values are shown. Isolate 4 = *Arthrobacter sps*

By monitoring the depreciable changes in LL-37 potency for *E. coli*, we can evaluate the effectiveness of NTM in neutralizing LL-37 activity. *E. coli* was inoculated into the LL-37-MABS culture supernatants remaining after 96-h. All MABS isolates tested inactivated 25 μg/ml of LL-37 at 37°C (data not shown), but only Isolate 2 neutralized the antimicrobial activity of both 25 and 150 μg/ml of LL-37 as noted by the overgrowth of *E. coli* (Figure 5c). For comparison, results from Isolate 2 and 8 are shown (Figure 5c). On the other hand, despite exposure of LL-37 to *Arthrobacter* for 96 h, the peptide remained potently active against *E. coli* when performed at 22°C (Figure S4d) compared to 37°C (Figure S4c).

DISCUSSION

Considering the SARS-CoV-2 (COVID-19) pandemic, there is a consequential need to better understand the virulence of respiratory microbes. Already, co-infection with MABS and SARS-CoV-2 has been reported in an elderly patient with multiple myeloma (Rodriguez et al., 2021). As a shapeshifter of the mycobacterial world, MABS displays a spectrum of morphologies and variations in their capacity to form pellicles or cord, but it's not known whether these morphotypes contribute to virulence and pathogenicity (Ryan & Byrd, 2018). Moreover, recovering MABS from the environment is difficult (Thomson et al., 2013). As a consequence, comparative virulence studies between environmental and clinical MABS isolates are scant. In this study, three different environmental MABS isolates recovered from natural sources such as freshwater biofilms or soil were used to infect a variety of cell models *in vitro* and these results were compared to three sputum-derived clinical MABS isolates.

Modest differences in the recovery of intracellular MABS was observed from amoebae or human epithelial cells (Figure 2b,c). We have previously shown isolates of slow-growing *Mycobacterium chimaera* demonstrate varied survival in human AM and THP-1 macrophages (Honda et al., 2019). In this study, similar CFU was recovered between the MABS isolates tested in both AM and THP-1 macrophages (Figures 2d and 3a). However, sputum-derived MABS Isolate 2 with rough morphology emerged as both a pellicle and cord former (Figures 1b,c and 3C). In addition, this isolate showed sustained CFU in the human models tested, induced high and prolonged production of pro-inflammatory cytokines from THP-1

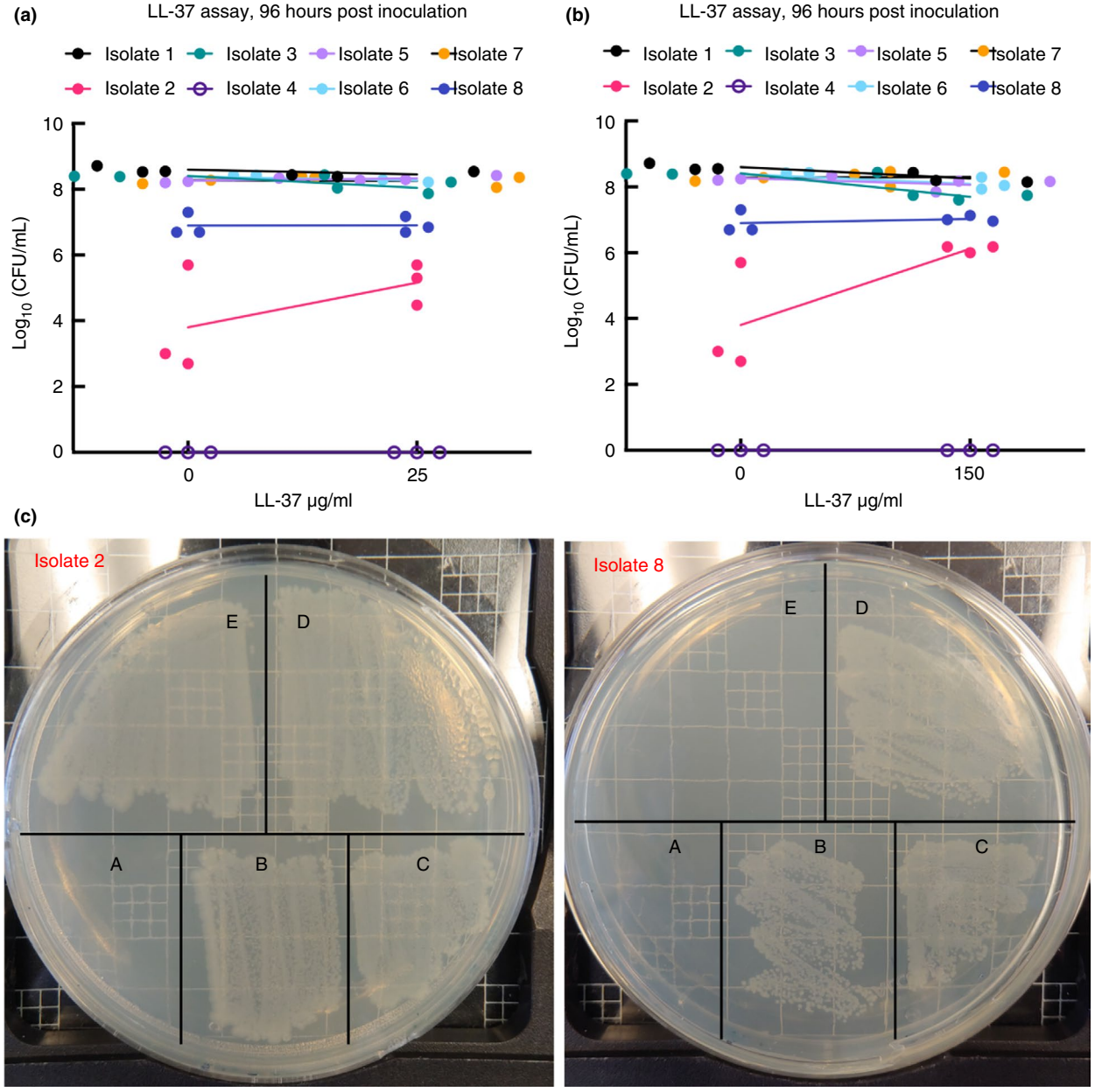

FIGURE 5 Resistance and inactivation of LL-37. The isolate panel was incubated in the presence of 0, 25 or 150 µg/ml of synthetic LL-37 peptide. Change in CFU between the 0 and 25 (a) or 0 and 150 µg/ml (b) of synthetic LL-37 at 96 h post exposure are reported. $n = 3$ independent experiments. (c) *Escherichia coli* bioassays were used to assess the potency of LL-37 remaining in culture after 96 h of incubation with MABS isolates or *Arthrobacter*. Representative images of Isolate 2 and 8 are shown. For these images, A = *E. coli* +25 µg/ml LL-37. B = *E. coli* alone. C = *E. coli*+vehicle (0.1% TFA). D = *E. coli* incubated in MABS culture supernatants with 25 µg/ml of LL-37 after 96 h. E = *E. coli* incubated in MABS culture supernatants with 150 µg/ml of LL-37 after 96 h. Isolate 4 = *Arthrobacter sp*

cells, as well as resisted and inactivated the antimicrobial activity of the host-protective peptide LL-37, suggesting it is a MABS of higher virulence compared to the other MABS isolates tested in this study. A limitation is that the disease status of the individuals from which sputum isolates were derived was not known at the time this study was performed.

A unique comparison was the inclusion of the MABS type strain ATCC 19977 and an innocuous, non-NTM bacterium, *Arthrobacter*. While there are a few reports of *Arthrobacter sp*. in the clinical microbiology literature (Mages et al., 2008), *Arthrobacter* is one of the most common indigenous, aerobic bacteria in soil ecosystems and used in a variety of bioremediation processes (Mongodin et al., 2006). The isolate of *Arthrobacter sp*. used was recovered from a similar environment as the non-clinical MABS isolates and was included to contextualize MABS virulence. In all cases, the replication of *Arthrobacter*

was inconsequential due to its sensitivity to human body temperature and antibiotics in cell culture media. Its inclusion, however, supports the general vigor of MABS in causing sustained infection in relevant environmental amoebae and human cell models of the lung. We also discovered robust production of TNFα by epithelial cells and AM in response to *Arthrobacter* (Figure 4a,b). Higher TNFα levels have also been reported by infected THP-1 cells in response to non-pathogenic bacteria including *Mycobacterium smegmatis* when compared to MABS ATCC 19977, suggesting TNFα, at minimum, is an important host defense mechanism against non-virulent bacteria (Feng et al., 2020). A prior study by Beltan et al. (2000) also reported non-pathogenic NTM induce greater levels of TNFα in human monocyte-derived macrophages than pathogenic NTM.

Multiplex analyte analyses was performed between the three environmental and three sputum isolates of MABS and *Arthrobacter* using THP-1 culture supernatants. Data in Figure S3 show robust TNFα and IL-6 production by *Arthrobacter* infected cells 24 h post infection that mirrored the immune response by environmental MABS infected THP-1 cells. By comparison, less cytokine mediators were produced in response to the clinical MABS isolates across the timepoints tested. Our data indicate that IL-8 is not a chemokine of significance for MABS THP-1 infected cells. However, others have used the release of IL-8 is a readout for toll-like receptor stimulation in MABS infected epithelial cells (Davidson et al., 2011). A limitation is that multiplex analyte studies could only be performed on the culture supernatants from THP-1 infected cells and should also be quantified using supernatants from epithelial cells and AM infected with the isolate panel at the same timepoints in future work.

AMP are potent, endogenous antibiotics produced by a variety of organisms and are important to innate defense against microbes. To understand the value of AMP against mycobacteria, 12 different AMP (including AMP from toads, wasps, and worms) were tested in a separate study, showing modest activity against slow-growing isolates of *Mycobacterium tuberculosis* (*Mtb*) and *Mycobacterium avium* (Portell-Buj et al., 2019). A cattle-derived AMP, indolocin, exhibited inhibitory activity at 128 μg/ml and the remaining AMP showed minimal inhibitory concentrations of >128 μg/ml. Human neutrophil peptides have been more widely studied in the context of mycobacteria (Gutsmann, 2016) with bactericidal activity against *Mtb*, *M. avium*, and *M. intracellulare* (Sharma et al., 2000). LL-37 is a cationic AMP with potent activity against Gram-negative and Gram-positive bacteria (Durr et al., 2006). We previously reported that LL-37 resistance and inactivation are dependent on the NTM isolate tested (Honda et al., 2019). In the current study, the inclusion of *Arthrobacter* strengthens the case for increased virulence of MABS, both environmental and clinical isolates, in the evasion of AMP produced by immune cells. That is, *Arthrobacter* was both susceptible to LL-37 and could not neutralize its activity (Figure S4). Comparably, all MABS isolates tested were resistant to LL-37 and all showed inactivation of 25 μg/ml of LL-37, the concentration sufficient to kill both the Gram-negative bacteria tested (*i.e. E. coli* and *Arthrobacter*). MABS Isolate 2 was the only isolate that demonstrated the capacity to inactivate the 150 μg/ml concentration of LL-37 (Figure 5). While the mechanism of LL-37 inactivation is not known, it is likely to involve polar phospholipids from the MABS cell wall (Honda et al., 2019).

This work has a few important implications. First, our prior work suggested that NTM isolates show varying interspecies, but also, intraspecies differences in terms of infectivity in host macrophages, particularly in the context of *M. chimaera* (Honda et al., 2019). The prior study also examined two different environmental MABS isolates which demonstrated relatively equivalent survival in THP-1 macrophages compared to another clinical MABS isolate. Important intraspecies differences among MABS, particularly in the context of Isolate 2, were observed in this study, urging for the consideration that NTM isolates should not be viewed as equivalently virulent even among clinical isolates. Second, the data presented also align with prior reports of rough MABS variants as more infectious than smooth isolates (Roux et al., 2016). Third, recent studies of MABS core and accessory genomes have brought to the forefront the emergence and description of genetically similar MABS clusters referred as "dominant circulating clones" (Bryant et al., 2016; Davidson, 2018). In the future, it would be useful to perform whole genome comparisons of environmental MABS isolates to better understand the distribution of MABS clones in environments worldwide. Fourth, the ability to form pellicles, to cord, and to resist and inactivate LL-37 by Isolate 2 was not sufficient to promote enhanced survival in the single eukaryotic cell models tested, but may prove consequential in an animal model. Thus, to fully understand virulence and pathogenicity differences between environmental and clinical MABS isolates, expanded studies in animal are urged.

The novel aspect of this work was the testing of both environmental and clinical isolates of MABS. However, this study has limitations including the low number of isolates tested. Examination of a larger panel should be performed to determine whether our findings translate to a larger sampling of environmental and clinical MABS isolates. In addition, the environmental isolates used were collected from a single geographic location in the United States; thus, follow up studies are needed using clinical and environmental MABS isolates from

other global locales to fully grasp the overarching pathogenesis of MABS.

In closing, this work begins to fill a current gap in knowledge by studying the consequence of environmental MABS infection using isolates recovered from a showerhead biofilm, freshwater stream, and soil in comparison to clinical MABS isolates and logically creates a foundation to expand other work related to the host and MABS factors that contribute to the progression of infection.

ACKNOWLEDGEMENTS

JRH acknowledges support from the Padosi Foundation. The funders had no role in the study design, data collection and interpretation, or the decision to submit the work for publication.

CONFLICT OF INTEREST

Authors declare that the research was conducted in the absence of any commercial or financial relationships that could be construed as a potential conflict of interest.

ORCID

Jennifer R. Honda https://orcid.org/0000-0002-4943-8738

REFERENCES

Adékambi, T., Ben Salah, S., Khlif, M., Raoult, D. & Drancourt, M. (2006) Survival of environmental mycobacteria in *Acanthamoeba polyphaga*. *Applied and Environment Microbiology*, 72, 5974–5981.

Adekambi, T., Colson, P. & Drancourt, M. (2003) rpoB-based identification of nonpigmented and late-pigmenting rapidly growing mycobacteria. *Journal of Clinical Microbiology*, 41, 5699–5708.

Beltan, E., Horgen, L. & Rastogi, N. (2000) Secretion of cytokines by human macrophages upon infection by pathogenic and non-pathogenic mycobacteria. *Microbial Pathogenesis*, 28, 313–318.

Bogdanovski, K., Chau, T., Robinson, C.J., MacDonald, S.D., Peterson, A.M., Mashek, C.M. et al. (2020) Antibacterial activity of high-dose nitric oxide against pulmonary *Mycobacterium abscessus* disease. *Access Microbiology*, 2, acmi000154.

Bryant, J.M., Grogono, D.M., Greaves, D., Foweraker, J., Roddick, I., Inns, T. et al. (2013) Whole-genome sequencing to identify transmission of *Mycobacterium abscessus* between patients with cystic fibrosis: a retrospective cohort study. *Lancet*, 381, 1551–1560.

Bryant, J.M., Grogono, D.M., Rodriguez-Rincon, D., Everall, I., Brown, K.P., Moreno, P. et al. (2016) Emergence and spread of a human-transmissible multidrug-resistant nontuberculous mycobacterium. *Science*, 354, 751–757.

Byrd, T.F. & Lyons, C.R. (1999) Preliminary characterization of a *Mycobacterium abscessus* mutant in human and murine models of infection. *Infection and Immunity*, 67, 4700–4707.

Ciampa, C. & Wong, K.S. (2021) *Mycobacterium abscessus* soft tissue infection: a rare and unusual cluster of presentations to a rural surgical service. *ANZ Journal of Surgery*, 91, 460–462.

Cook, J.L. (2010) Nontuberculous mycobacteria: opportunistic environmental pathogens for predisposed hosts. *British Medical Bulletin*, 96, 45–59.

Davidson, L.B., Nessar, R., Kempaiah, P., Perkins, D.J. & Byrd, T.F. (2011) *Mycobacterium abscessus* glycopeptidolipid prevents respiratory epithelial TLR2 signaling as measured by HbetaD2 gene expression and IL-8 release. *PLoS One*, 6, e29148.

Davidson, R.M. (2018) A closer look at the genomic variation of geographically diverse *Mycobacterium abscessus* clones that cause human infection and disease. *Frontiers in Microbiology*, 9, 2988.

Dedrick, R.M., Guerrero-Bustamante, C.A., Garlena, R.A., Russell, D.A., Ford, K., Harris, K. et al. (2019) Engineered bacteriophages for treatment of a patient with a disseminated drug-resistant *Mycobacterium abscessus*. *Nature Medicine*, 25, 730–733.

Degiacomi, G., Sammartino, J.C., Chiarelli, L.R., Riabova, O., Makarov, V. & Pasca, M.R. (2019) *Mycobacterium abscessus*, an emerging and worrisome pathogen among cystic fibrosis patients. *International Journal of Molecular Sciences*, 20(23), 5868.

Durr, U.H., Sudheendra, U.S. & Ramamoorthy, A. (2006) LL-37, the only human member of the cathelicidin family of antimicrobial peptides. *Biochimica et Biophysica Acta*, 1758, 1408–1425.

Epperson, L.E. & Strong, M. (2020) A scalable, efficient, and safe method to prepare high quality DNA from mycobacteria and other challenging cells. *Journal of Clinical Tuberculosis and Other Mycobacterial Diseases*, 19, 100150.

Falkinham, J.O. 3rd (2009) Surrounded by mycobacteria: nontuberculous mycobacteria in the human environment. *Journal of Applied Microbiology*, 107, 356–367.

Feng, Z., Bai, X., Wang, T., Garcia, C., Bai, A., Li, L. et al. (2020) Differential responses by human macrophages to infection with *Mycobacterium tuberculosis* and non-tuberculous mycobacteria. *Frontiers in Microbiology*, 11, 116.

Gupta, R.S., Lo, B. & Son, J. (2018) Phylogenomics and comparative genomic studies robustly support division of the genus mycobacterium into an emended genus mycobacterium and four novel genera. *Frontiers in Microbiology*, 9, 1–41.

Gutsmann, T. (2016) Interaction between antimicrobial peptides and mycobacteria. *Biochimica et Biophysica Acta*, 1858, 1034–1043.

Hasan, N.A., Norton, G.J., Virdi, R., Epperson, L.E., Vang, C.K., Hellbusch, B. et al. (2021) Measurable genomic changes in *Mycobacterium avium* subsp. hominissuis after long-term adaptation in *Acanthamoeba lenticulata* and reduced persistence in macrophages. *Journal of Bacteriology*, 203(6), 1–15.

Hobro, A.J. & Smith, N.I. (2017) An evaluation of fixation methods: spatial and compositional cellular changes observed by Raman imaging. *Vibrational Spectroscopy*, 91, 31–45.

Honda, J.R., Hasan, N.A., Davidson, R.M., Williams, M.D., Epperson, L.E., Reynolds, P.R. et al. (2016) Environmental nontuberculous mycobacteria in the Hawaiian Islands. *PLoS Neglected Tropical Diseases*, 10, e0005068.

Honda, J.R., Hess, T., Carlson, R., Kandasamy, P., Nieto Ramirez, L.M., Norton, G.J. et al. (2019) Nontuberculous mycobacteria show differential infectivity and use phospholipids to antagonize LL-37. *American Journal of Respiratory Cell and Molecular Biology*, 62(3), 354–363.

Honda, J., Hess, T., Malcolm, K., Ovrutsky, A., Bai, X., Irani, V. et al. (2015) Pathogenic nontuberculous mycobacteria resist and inactivate cathelicidin: implication of a novel role for polar mycobacterial lipids. *PLoS One*, 10(5), e0126994.

Imam, O., Al-Zubaidi, K., Janahi, M., Imam, A., Leghrouz, B., Dobson, S. et al. (2021) Peritoneal dialysis-associated peritonitis caused by *Mycobacterium abscessus* in children-a case report. *Open Forum Infectiosus Disease*, 8, ofaa579.

Kim, A.Y., Davis, A.S., Moreau, A., Drevets, D.A. & Melendez, D.P. (2020) Management of nontuberculous mycobacterial infections of the eye and orbit: a retrospective case series. *American Journal of Ophthalmology Case Reports*, 20, 100971.

Lehrer, R.I. & Ganz, T. (2002) Cathelicidins: a family of endogenous antimicrobial peptides. *Current Opinion in Hematology*, 9, 18–22.

Lobocka, M., Dabrowska, K. & Gorski, A. (2021) Engineered bacteriophage therapeutics: rationale, challenges and future. *BioDrugs: Clinical Immunotherapeutics, Biopharmaceuticals and Gene Therapy*, 35, 255–280.

Lopeman, R.C., Harrison, J., Desai, M. & Cox, J.A.G. (2019) *Mycobacterium abscessus: environmental bacterium turned clinical nightmare*. *Microorganisms*, 7, 1–17.

Mages, I.S., Frodl, R., Bernard, K.A. & Funke, G. (2008) Identities of Arthrobacter spp. and Arthrobacter-like bacteria encountered in human clinical specimens. *Journal of Clinical Microbiology*, 46, 2980–2986.

Martiniano, S.L., Nick, J.A. & Daley, C.L. (2019) Nontuberculous mycobacterial infections in cystic fibrosis. *Thoracic Surgery Clinics*, 29, 95–108.

Mongodin, E.F., Shapir, N., Daugherty, S.C., DeBoy, R.T., Emerson, J.B., Shvartzbeyn, A. et al. (2006) Secrets of soil survival revealed by the genome sequence of *Arthrobacter aurescens* TC1. *PLoS Genetics*, 2, e214.

Nessar, R., Cambau, E., Reyrat, J.M., Murray, A. & Gicquel, B. (2012) *Mycobacterium abscessus*: a new antibiotic nightmare. *Journal of Antimicrobial Chemotherapy*, 67(4), 810–818

Patel, O.A., Bakhshi, G.D., Nadkarni, A.R. & Rangwala, Z.S. (2021) Granulomatous mastitis due to non-tuberculous mycobacteria: a diagnostic and therapeutic dilemma. *Clinics and Practice*, 11, 228–234.

Portell-Buj, E., Vergara, A., Alejo, I., Lopez-Gavin, A., Monte, M.R., San Nicolas, L. et al. (2019) In vitro activity of 12 antimicrobial peptides against *Mycobacterium tuberculosis* and *Mycobacterium avium* clinical isolates. *Journal of Medical Microbiology*, 68, 211–215.

Rodriguez, J.A., Bonnano, C., Khatiwada, P., Roa, A.A., Mayer, D. & Eckardt, P.A. (2021) COVID-19 coinfection with *Mycobacterium abscessus* in a patient with multiple myeloma. *Case Reports in Infectious Diseases*, 2021, 8840536.

Roux, A.L., Viljoen, A., Bah, A., Simeone, R., Bernut, A., Laencina, L. et al. (2016) The distinct fate of smooth and rough Mycobacterium abscessus variants inside macrophages. *Open Biology*, 6, 1–12.

Ryan, K. & Byrd, T.F. (2018) *Mycobacterium abscessus*: shapeshifter of the mycobacterial world. *Frontiers in Microbiology*, 9, 2642.

Sharma, S., Verma, I. & Khuller, G.K. (2000) Antibacterial activity of human neutrophil peptide-1 against *Mycobacterium tuberculosis* H37Rv: in vitro and ex vivo study. *European Respiratory Journal*, 16, 112–117.

Stecher, G., Tamura, K. & Kumar, S. (2020) Molecular evolutionary genetics analysis (MEGA) for macOS. *Molecular Biology and Evolution*, 37, 1237–1239.

Telenti, A., Marchesi, F., Balz, M., Bally, F., Bottger, E.C. & Bodmer, T. (1993) Rapid identification of mycobacteria to the species level by polymerase chain reaction and restriction enzyme analysis. *Journal of Clinical Microbiology*, 31, 175–178.

Thomas, V. & McDonnell, G. (2007) Relationship between mycobacteria and amoebae: ecological and epidemiological concerns. *Letters in Applied Microbiology*, 45, 349–357.

Thomson, R.M., Carter, R., Tolson, C., Coulter, C., Huygens, F. & Hargreaves, M. (2013) Factors associated with the isolation of Nontuberculous mycobacteria (NTM) from a large municipal water system in Brisbane, Australia. *BMC Microbiology*, 13, 89.

Virdi, R., Lowe, M.E., Norton, G.J., Dawrs, S.N., Hasan, N.A., Epperson, L.E. et al. (2021) Lower recovery of nontuberculous mycobacteria from outdoor Hawai'i environmental water biofilms compared to indoor samples. *Microorganisms*, 9, 224.

Wojcik, B.M., Mitchell, J.D., Chong, T. & Rove, J.Y. (2021) Management of refractory *Mycobacterium abscessus* sternal infection following reoperative cardiac surgery. *Clinical Case Reports*, 9, 2328–2331.

Yonekawa, A., Miyake, N., Minami, J., Murakami, D., Fukano, H., Hoshino, Y. et al. (2020) Parotitis caused by *Mycobacteroides abscessus* subspecies abscessus. *Auris, Nasus, Larynx*, 22(4), 1–4.

Zanetti, M. (2004) Cathelicidins, multifunctional peptides of the innate immunity. *Journal of Leukocyte Biology*, 75, 39–48.

SUPPORTING INFORMATION

Additional supporting information may be found in the online version of the article at the publisher's website.

How to cite this article: Vang, C.K., Dawrs, S.N., Oberlag, N.M., Gilmore, A.E., Hasan, N.A. & Honda, J.R. (2022) Comparative survival of environmental and clinical *Mycobacterium abscessus* isolates in a variety of diverse host cells. *Journal of Applied Microbiology*, 132, 3302–3314. https://doi.org/10.1111/jam.15416